Nanoscale Self-Assemblies in Biological Molecules:

Structures and Interactions of Microtubules and Microtubule-Associated-Molecules

PART II

Multi-length scale imaging of MTs

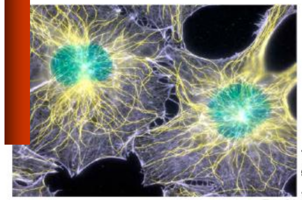

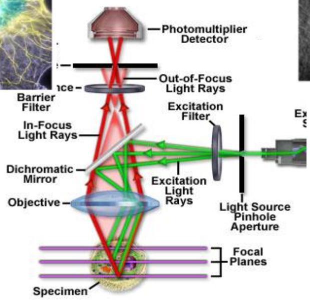

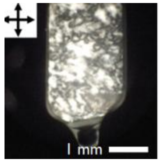

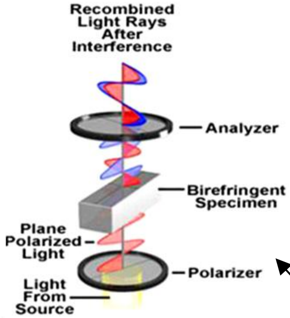

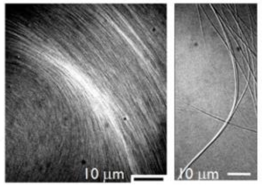

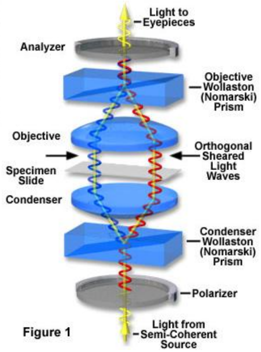

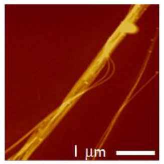

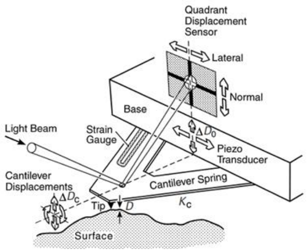

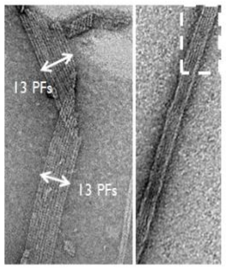

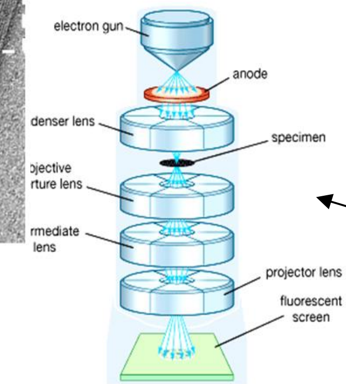

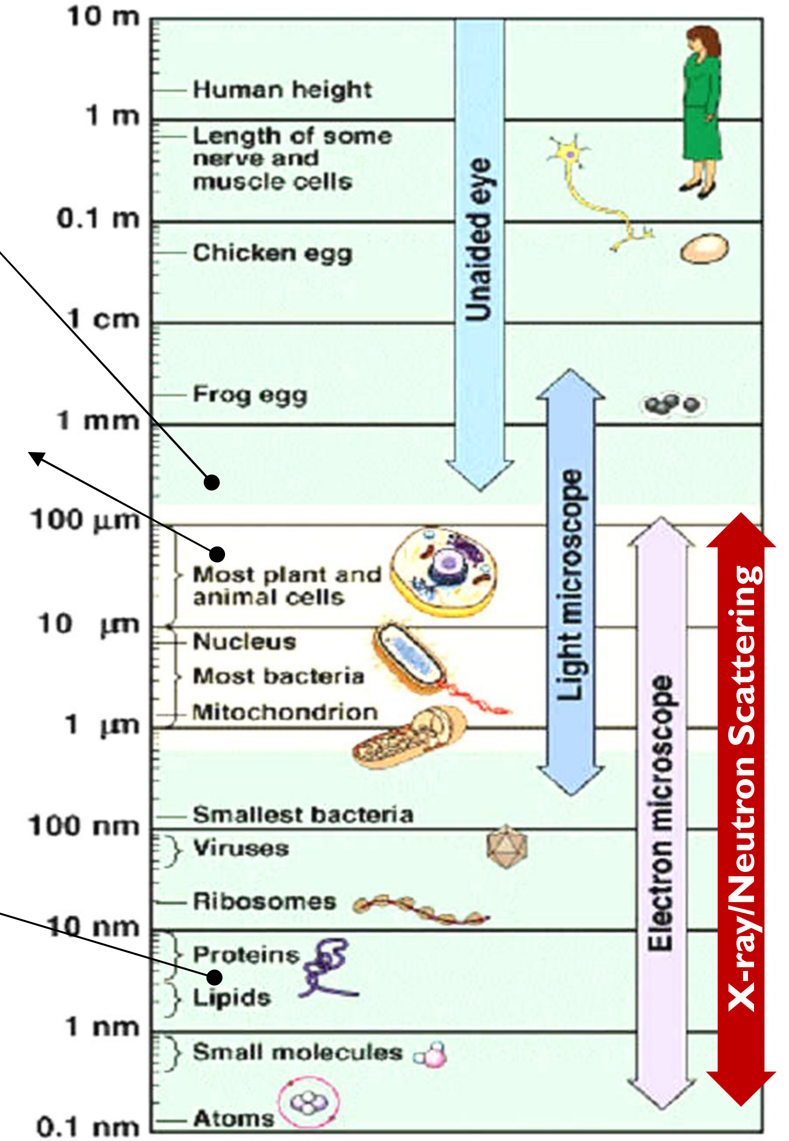

Light Microscope: Confocal Microscope

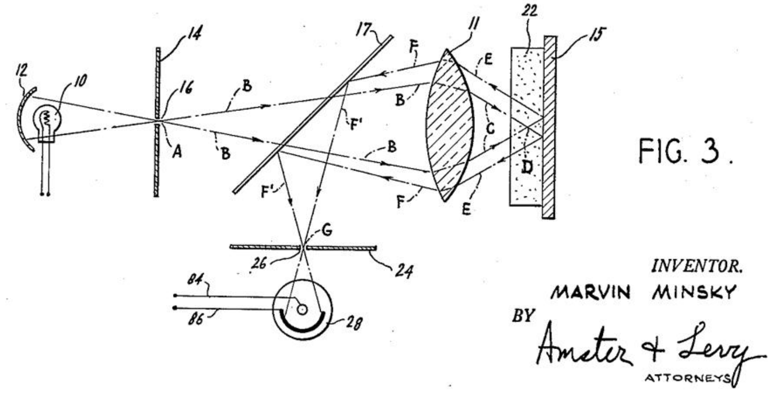

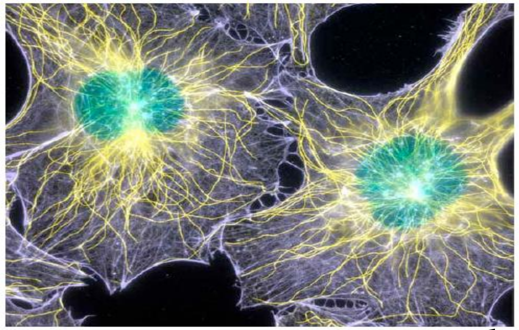

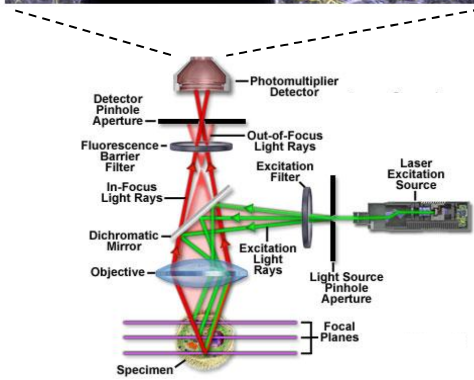

Marvin Lee Minsky is a cognitive scientist in the field of artificial intelligence (AI), co-founder of MIT's AI laboratory, and author of several texts on AI and philosophy. Minsky was an adviser on the movie 2001: A Space Odyssey (1968)

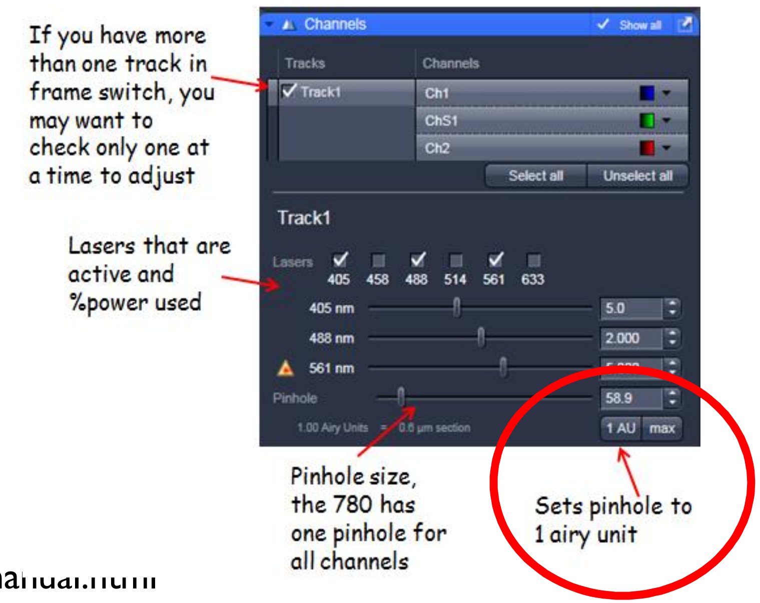

http://microscopy.duke.edu/780upmanual.html

X-ray Scattering: Convolution of Form Factor and Structure Factor

$$I \propto \int \left|F(q)\right|^2 d\Omega_q$$

$$F(Q) = \underbrace{\sum_{r_j} f_j(Q) e^{iQ\cdot r_j}}_{\text{Form factor}} \underbrace{\sum_{R_n} e^{iQ\cdot R_n}}_{\text{Structure factor}}$$

Form factor
: shape and size of object

Structure factor
: spacing and ordering structur between objects

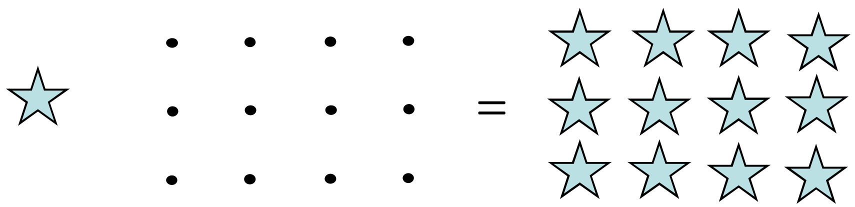

$$\mathcal{F}\{g\} = F(k)$$
$$\mathcal{F}\{h\} = H(k)$$
$$If\ g = f \otimes h\ ,$$
$$\mathcal{F}\{g\} = \mathcal{F}\{f \otimes h\} = \mathcal{F}\{f\} \cdot \mathcal{F}\{h\}$$
$$\text{or } G(k) = F(k)\, H(k)$$

$$\rightarrow \mathcal{F}\{f \otimes h\} = \int_{-\infty}^{\infty} g(X) e^{ikX} dX$$
$$= \int_{-\infty}^{\infty} e^{ikX} \left[\int_{-\infty}^{\infty} f(x) h(X-x) dx \right] dX$$

$$\text{Thus} \quad G(k) = \int_{-\infty}^{\infty} \left[\int_{-\infty}^{\infty} h(X-x) e^{ikX} dX \right] f(x) dx$$
$$w = X - x$$
$$G(k) = \underbrace{\int_{-\infty}^{\infty} f(x) e^{ikx} dx}_{F(k)} \underbrace{\int_{-\infty}^{\infty} h(w) e^{ikw} dw}_{H(k)}$$

SAXS reveals Assembly Structures of MTs

- Young's single slit experiment

The amplitude of the optical field at any point beyond is the superposition of all the secondary wavelets.

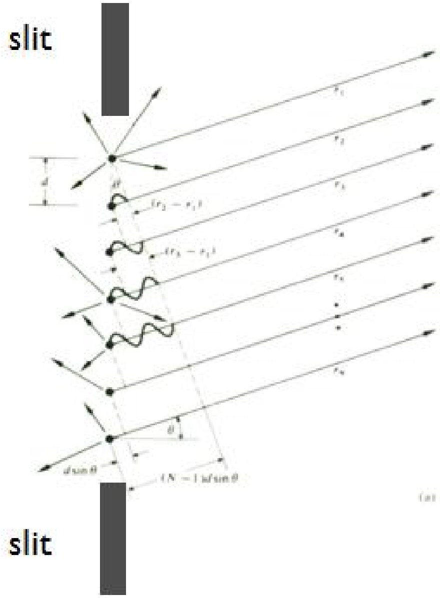

source strength per unit length $\varepsilon_L \equiv \frac{1}{D} \lim_{N \to \infty} (\varepsilon_0 N)$

$$dE = \frac{\varepsilon_L}{R} \sin(wt - kr)dy$$

§

$$r = R - y \sin\theta + (y^2 / 2R)\cos^2\theta + \cdots$$

$$E = \frac{\varepsilon L}{R} \int_{-b/2}^{b/2} \sin[wt - k(R - y\sin\theta)]dy$$

$$I(\theta) = \langle E^2 \rangle$$

$$I(\theta) = I(0)\left(\frac{\sin\beta}{\beta}\right)^2$$

$$\beta = (kb/2)\sin\theta$$

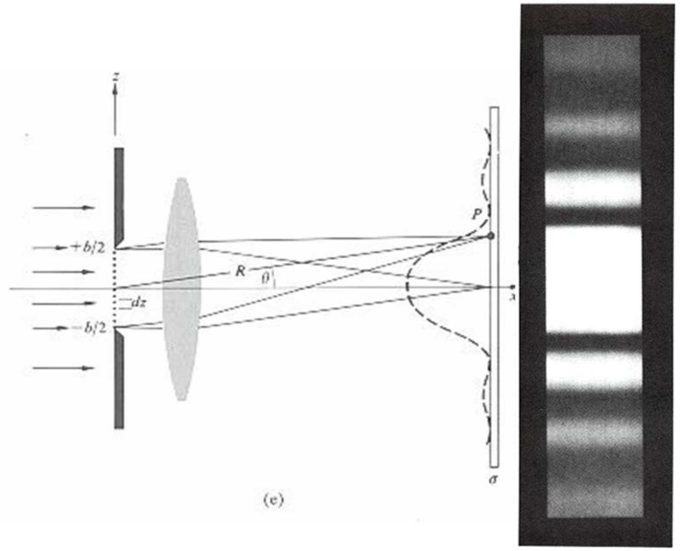

Hecht "Optics"

SAXS reveals Assembly Structures of MTs

- Young's double slit experiment

$$E \sim \int_{-b/2}^{b/2} \sin[\,wt - k(R - z\sin\theta)]dz + \int_{a-b/2}^{a+b/2} \sin[\,wt - k(R - z\sin\theta)]dz$$

$$\sim 2b(\frac{\sin\beta}{\beta})\cos\alpha\,\sin(wt - kR + \alpha)$$

$$I(\theta) = 4I_0(\frac{\sin\beta}{\beta})^2 \cos\alpha^2$$

$$\alpha = (ka/2)\sin\theta$$

$$\beta = (kb/2)\sin\theta$$

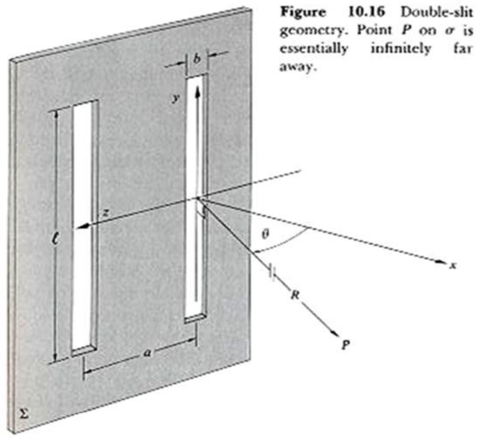

Figure 10.16 Double-slit geometry. Point P on σ is essentially infinitely far away.

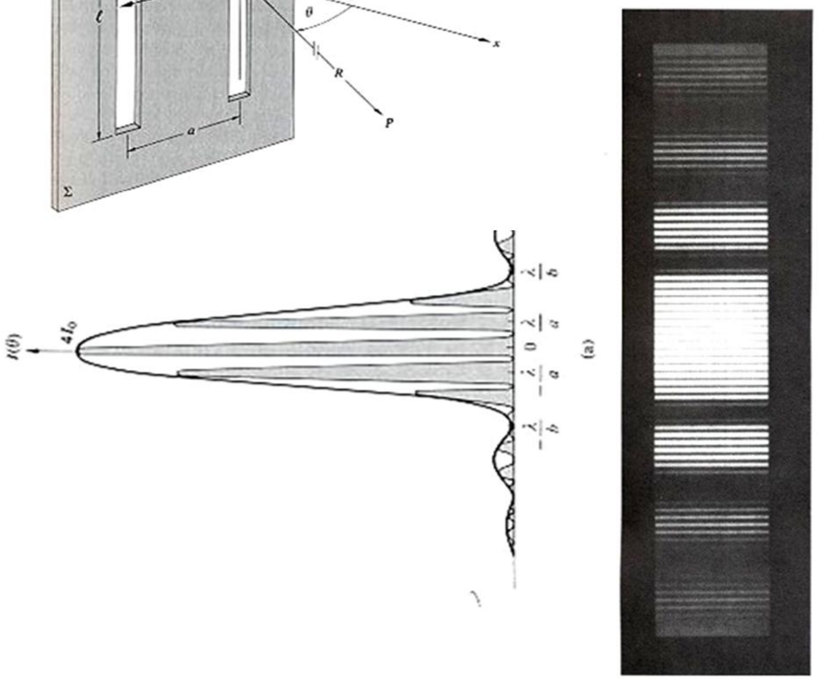

SAXS reveals Assembly Structures of MTs

- ➢ Diffraction by many slits

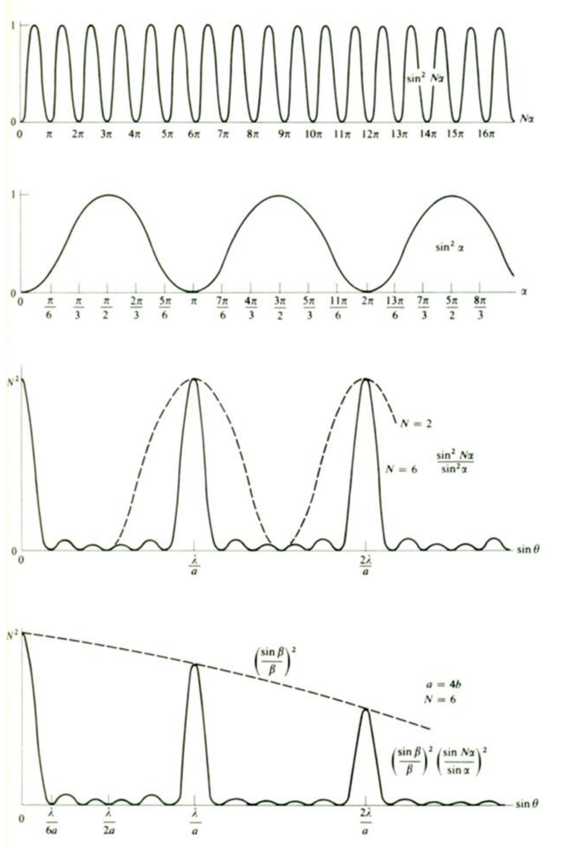

$$E \sim \int_{-b/2}^{b/2} \sin[wt - k(R - z\sin\theta)]\,dz + \int_{a-b/2}^{a+b/2} \sin[wt - k(R - z\sin\theta)]\,dz$$

$$+ \int_{2a-b/2}^{2a+b/2} \sin[wt - k(R - z\sin\theta)]\,dz + \cdots$$

$$+ \int_{(N-1)a-b/2}^{(N-1)a+b/2} \sin[wt - k(R - z\sin\theta)]\,dz$$

$$E \sim b\left(\frac{\sin\beta}{\beta}\right)\sin(wt - kR + 2\alpha j)$$

$$E = \sum_{j=0}^{N-1} E_j$$

$$E \sim \sum_{j=0}^{N-1} b\left(\frac{\sin\beta}{\beta}\right)\sin(wt - kR + 2\alpha j)$$

$$\sim b\left(\frac{\sin\beta}{\beta}\right)\left(\frac{\sin N\alpha}{\sin\alpha}\right)\sin[wt - kR + (N-1)\alpha]$$

$$I(\theta) = I_0\left(\frac{\sin\beta}{\beta}\right)^2\left(\frac{\sin N\alpha}{\sin\alpha}\right)^2$$

$$\alpha = (ka/2)\sin\theta$$

$$\beta = (kb/2)\sin\theta$$

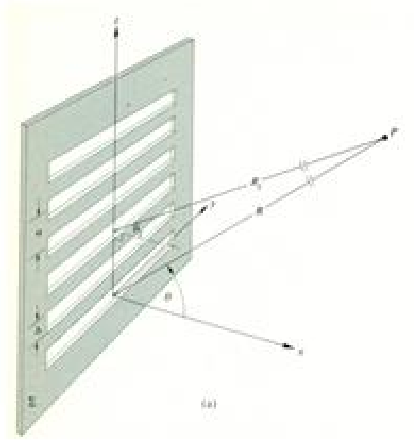

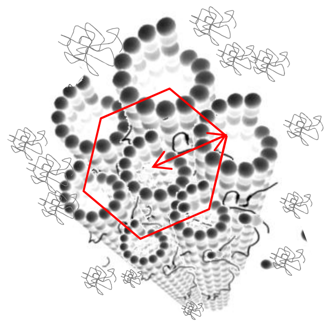

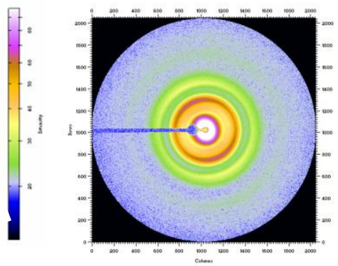

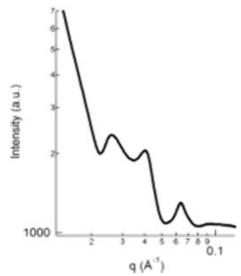

SAXS reveals Assembly Structures of MTs

$$I \propto \int |F(q)|^2 d\Omega_q$$

$$F(Q) = \underbrace{\sum_{r_j} f_j(Q) e^{iQ\cdot r_j}}_{\textit{Form factor}} \underbrace{\sum_{R_n} e^{iQ\cdot R_n}}_{\textit{Structure factor}}$$

Form factor : shape and size of object

Structure factor : spacing and ordering structure between objects

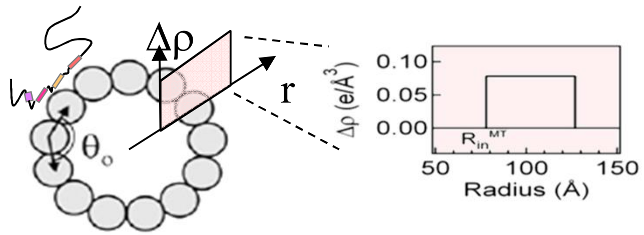

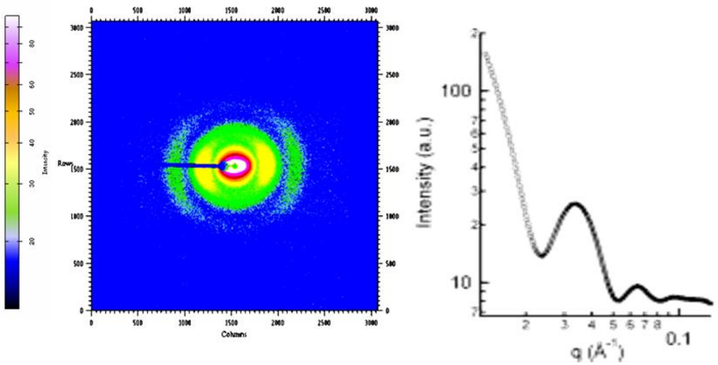

$$I \propto \int |F(q)|^2 d\Omega_q$$

$$F(q) \propto \int \Delta\rho_o(r) e^{-iq\,r} \propto 4\pi\Delta\rho_o \sin(Hq_z) q_z^{-1} \int_{R_i}^{R_o} \rho d\rho J_0(q_\perp \rho)$$

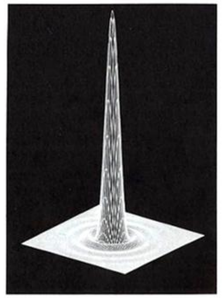

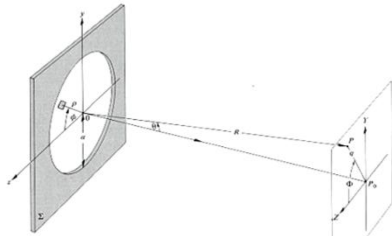

Figure 10.26 Circular aperture geometry.

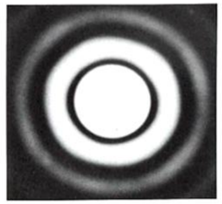

$$E = \frac{\varepsilon_A e^{i(wt-kR)}}{R} \iint_{Aperture} e^{i(Yy+Zz)/R} dS$$

$$z = \rho\cos\phi \qquad y = \rho\sin\phi$$

$$Z = q\cos\Phi \qquad Y = q\sin\Phi$$

$$E = \frac{\varepsilon_A e^{i(wt-kR)}}{R} \int_{\rho=0}^{a} \int_{\phi=0}^{2\pi} e^{i(k\rho q/R)} \cos(\phi-\Phi) \rho d\rho d\phi$$

$$= \frac{\varepsilon_A e^{i(wt-kR)}}{R} 2\pi \int_0^a J_0(k\rho q/R) \rho d\rho$$

$$= \frac{\varepsilon_A e^{i(wt-kR)}}{R} 2\pi a^2 (R/kaq) J_1(kaq/R)$$

$$I = I(0)\left[\frac{2J_1(ka\sin\theta)}{ka\sin\theta}\right]^2$$

Airy Disk, limit of resolution

Airy rings

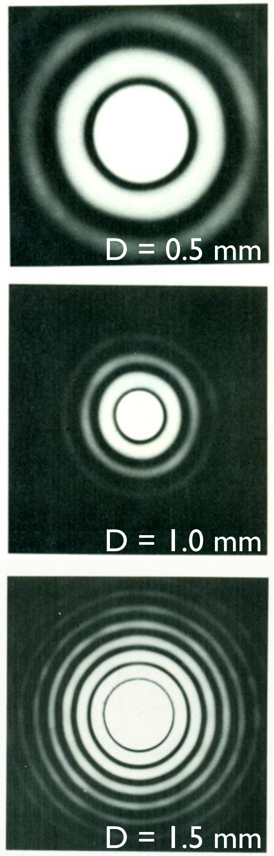

$$I = I(0)\left[\frac{2J_1(ka\sin\theta)}{ka\sin\theta}\right]^2$$

$J_1(u) = 0$ when $\Delta l_{min} = 1.22\dfrac{R\lambda}{a}$: the radius of the Airy disk

Δl is the center-to-center separation of the images.

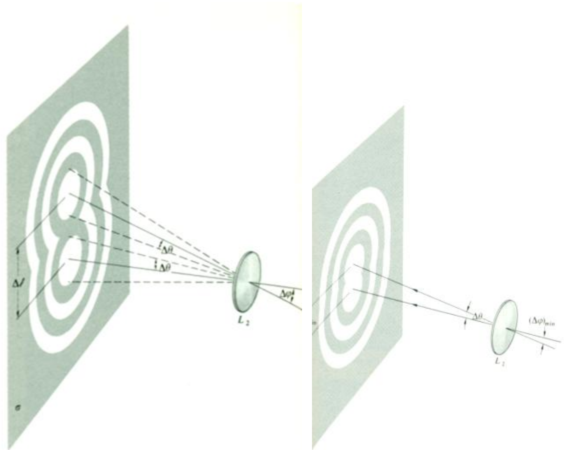

$1/(\Delta l)_{min}$: the resolving power

$(\Delta l)_{min} \sim \lambda$

: the electron microscope utilizes equivalent wavelength of about 10^{-4} to 10^{-5} of light.

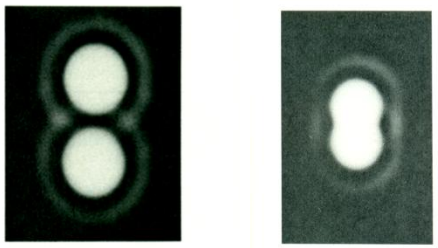

$(\Delta l)_{min} \sim 1/a$

: the Mount Palomer telescope has a mirror 5 m in diameter. At 550 nm it has an angular limit of resolution of 2.7×10^{-2}s of arc. In contrast, the human eye of 2 mm pupil, with λ = 550 nm, has 1 min of arc.

Small angle X-ray scattering (SAXS)

SAXS instrument provides cutting edge capabilities for probing large length scale structures such as polymers, biological macromolecules, meso- and nano-porous materials, and molecular self-assemblies.

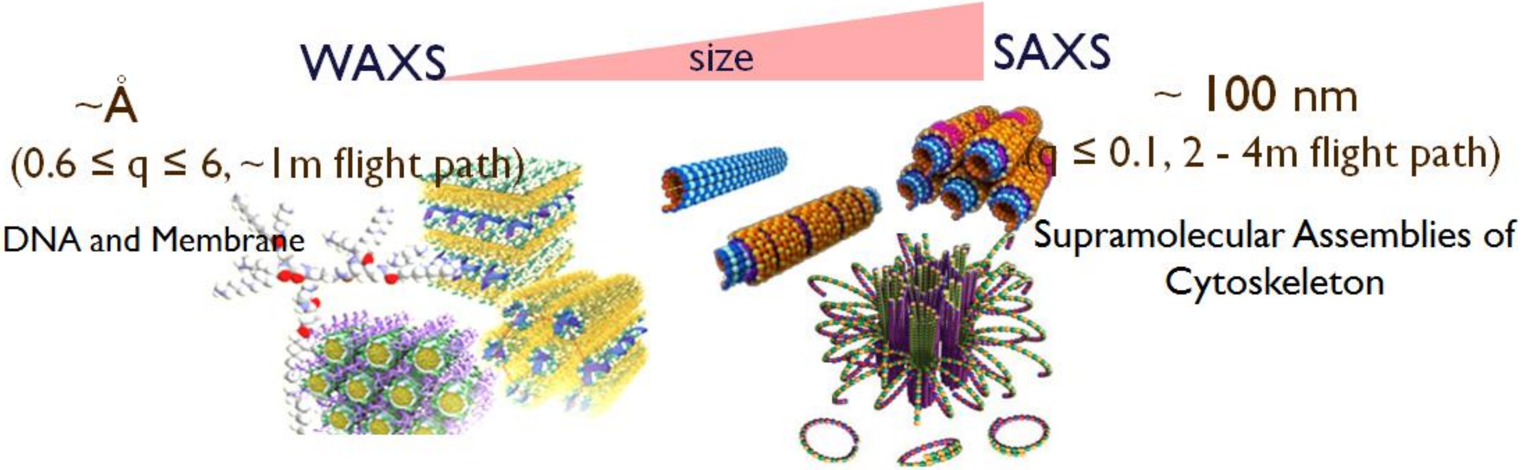

Synchrotron SAXS in BL-4C (PAL); 40M SANS (KAERI)

SAXS Study

(i) Tau is a molecular switch regulating the radial curvature of tubulin

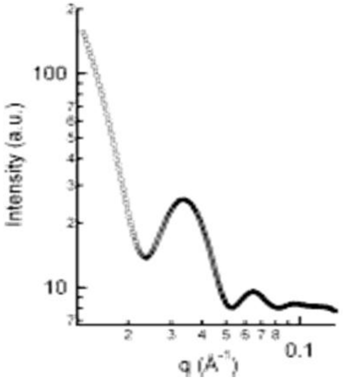

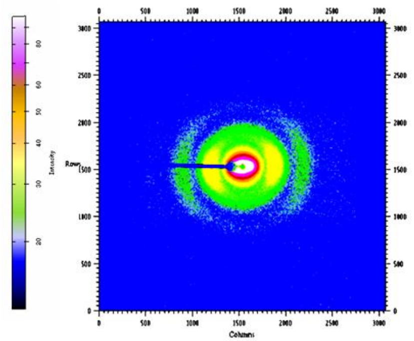

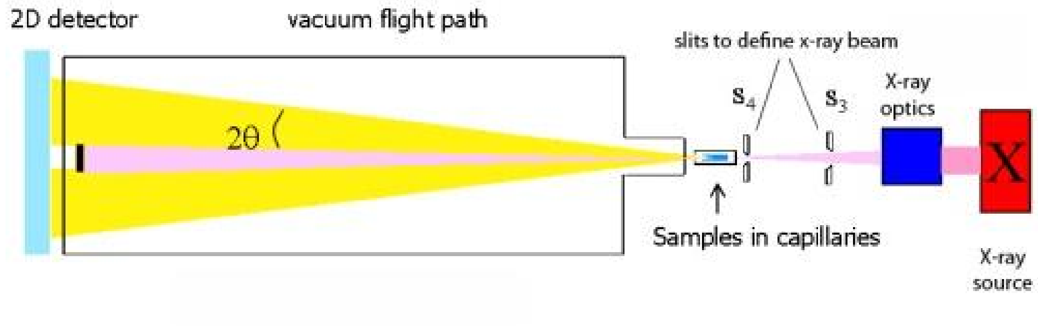

MT form factor

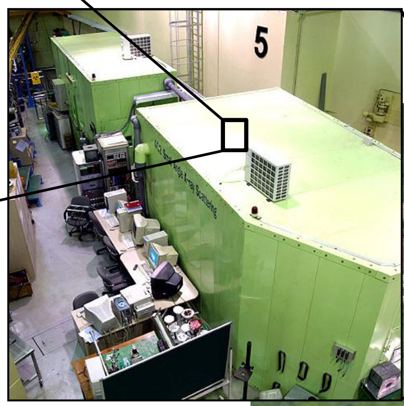

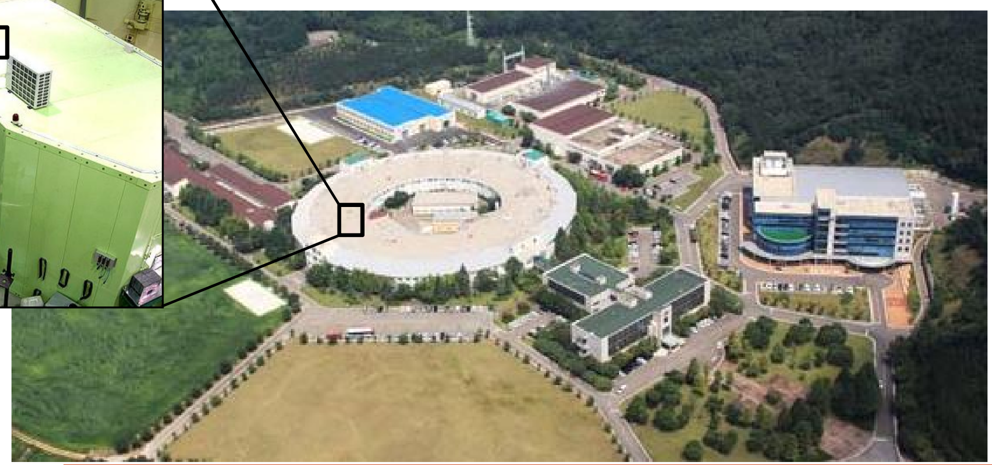

BL-4C SAXS II at PAL (Pohang Accelerator Laboratory)

SAXS Study

(i) Tau is a molecular switch regulating the radial curvature of tubulin

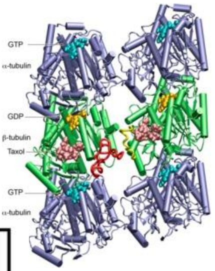

1st box

- The electron density $\Delta\rho_{tubulin}$ = 0.07817 electron/Å^3. (ρ_{water} = 0.33 electron/Å^3)
- The wall thickness 49 Å.

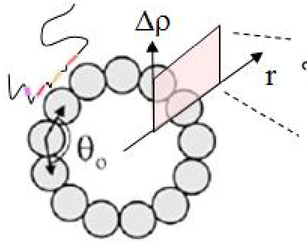

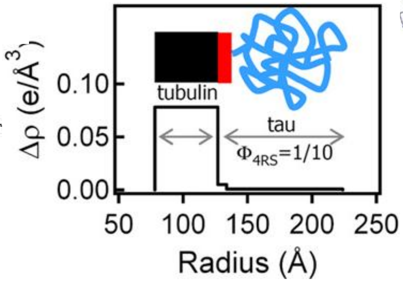

2nd box

- The diameter of tau d ≈ 6.88 Å.
- The mass density of tau 1.41 g/cc.
- $\Delta\rho_{tau}$ = 0.005 electron/Å^3 for Φ_{4RS} = 1/10 (ρ_{tau} = 0.462 electron/Å^3).

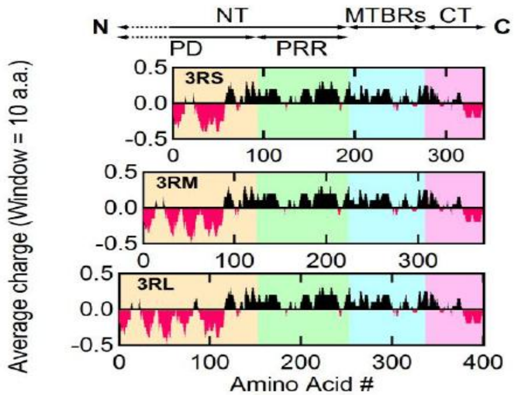

3rd box

- R_g = 1.927 $N^{0.6}$ = 41.2 Å for projection domain of short tau
- $\Delta\rho_{tau}$ = 0.0009 electron/Å^3

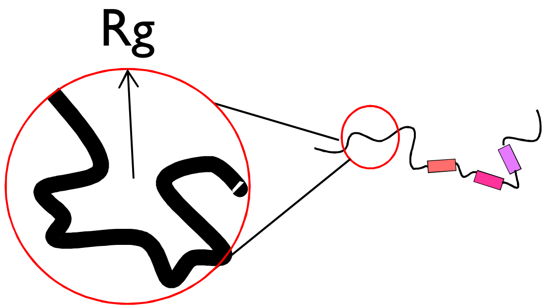

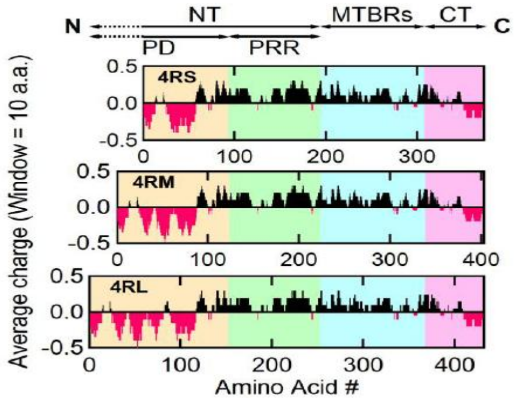

R_g of Denatured Proteins

➢ The dimensions of denatured proteins scale with polypeptide length by means of the power law relationship expected for random-coil behavior

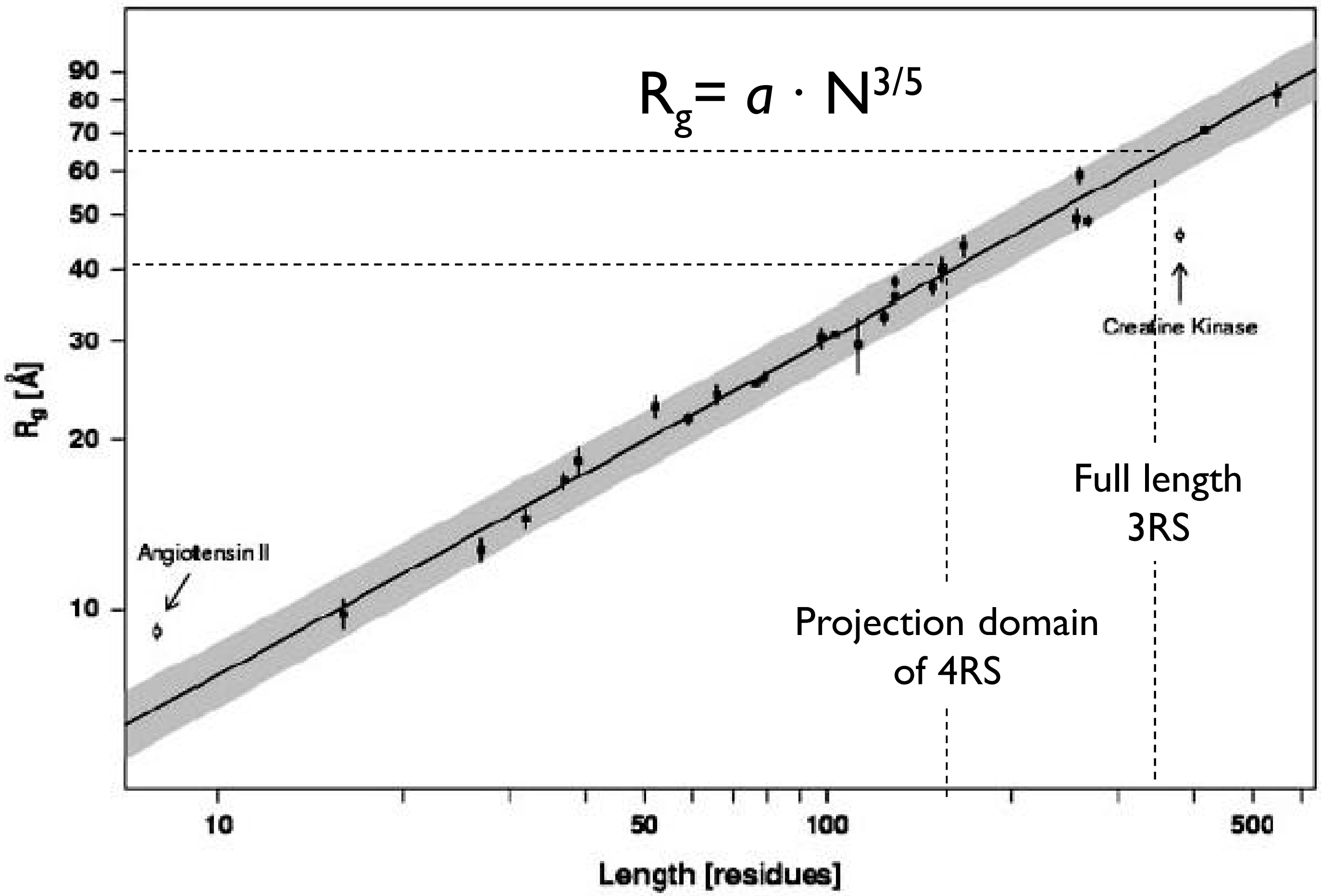

J. Kohn, K. Plexco, et al. PNAS, 101 (2004)

R_g of Denatured Proteins

- The dimensions of most chemically denatured proteins scale with polypeptide length by means of the power law relationship expected for random-coil behavior

Guinier Approximation

$$I(q) \cong I(0)e^{-\frac{1}{3}R_g^2q^2}$$

$$\ln[I(q)] \cong \ln[I(0)] - \frac{1}{3}R_g^2q^2$$

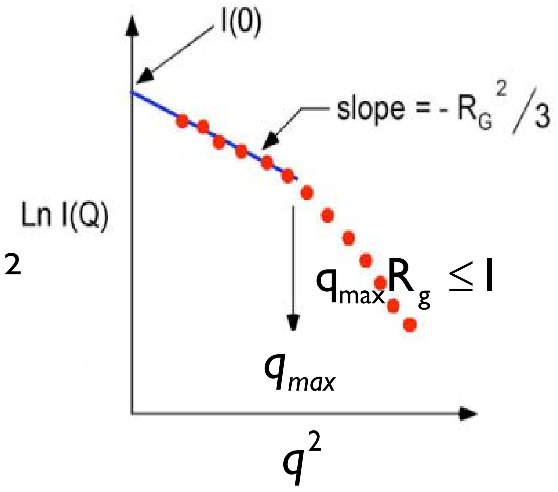

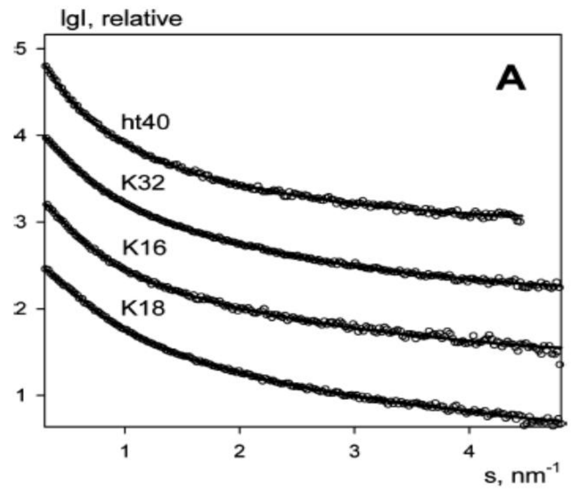

Table 1: Radii of Gyration

construct	no. of amino acids	experimental R_g (nm)	random coil R_g[a] (nm)	experimental R_g/RC R_g ratio	calculated R_g (PDB entry)[b]
ht40	441	6.5 ± 0.3	6.9	0.94	2.4 (1AQH)
K32	202	4.2 ± 0.3	4.4	0.96	1.8 (1AUN)
K16	174	3.9 ± 0.3	4.0	0.98	1.6 (1A33)
K18	130	3.8 ± 0.3	3.4	1.12	1.5 (8LYZ)
ht23	352	5.3 ± 0.3	6.1	0.88	2.1 (1AIR)
K27	171	3.7 ± 0.2	4.0	0.94	1.7 (1EUB)
K17	143	3.6 ± 0.2	3.6	1.02	1.8 (1J57)

Mandelkow, et al. Biochem (2008)

SAXS Study

(i) Tau is a molecular switch regulating the radial curvature of tubulin

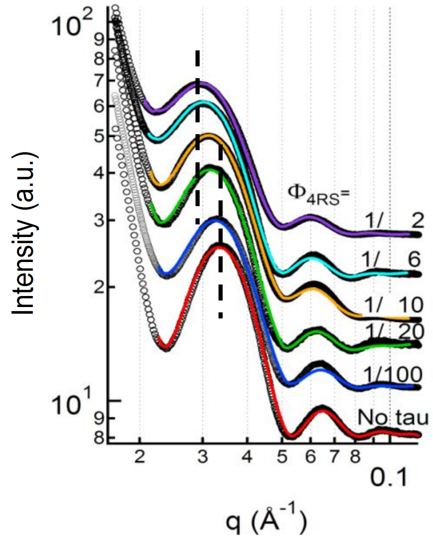

The electron density contrast between the layer of tau and water is negligible. Main parameter allowed to give the fit of x-ray data to this model is the inner radius of MTs $\langle R_{in}^{MT} \rangle$.

Shift in the mean number of PFs from 13 to 14. Non-integer values measured in X-ray imply a variation in the distribution of N_{pf} in MTs.

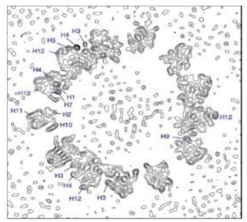

Figure 5. Contour Plot of One Section of the Microtubule Density Map

The section cuts through adjacent monomers 9.4 Å apart along the axis and is viewed looking from the plus end toward the minus end. Positions of several of the α helices in the crystal structure are marked.

$\langle N_{pf} \rangle$ = 13.5 implies there are equal numbers of MTs with either 13 or 14 protofilaments.

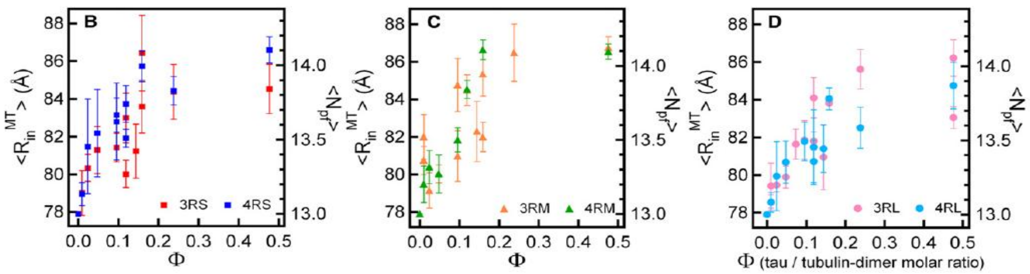

SAXS Study

(i) Tau is a molecular switch regulating the radial curvature of tubulin

The change in c_o of MTs by tau binding.

Main change in the radius occurs at low coverage of tau, for example, ~75 % change has occurred at 0.1, 10 % coverage of tau on the MT surface. ……….. Allosteric role of tau

KCl suppresses the electrostatic interaction between tau and MTs, resulting in desorption of tau molecules from MTs, and a decrease in the radius.

The electrostatic interaction is dominant for the attachment of tau to MTs.

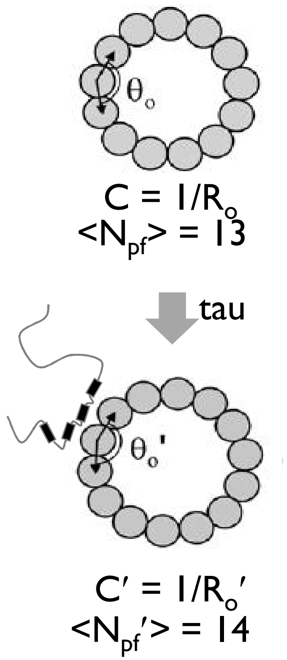

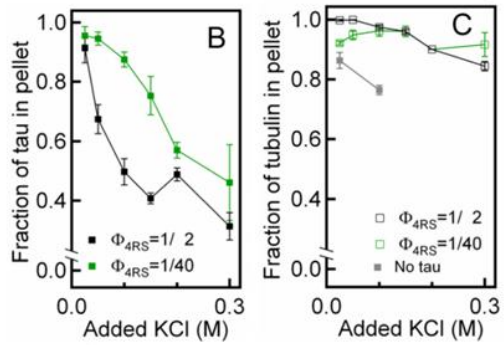

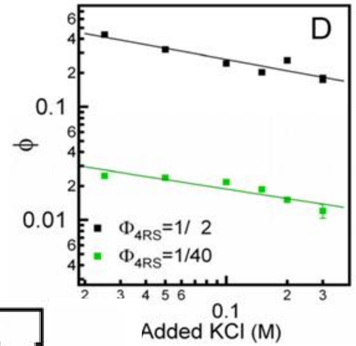

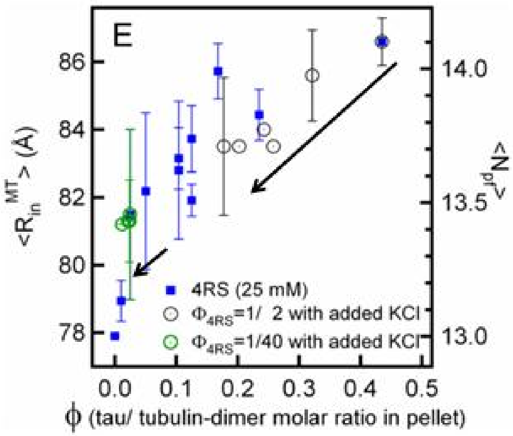

M.C. Choi, et al., Biophy. J. 97; 519 (2009)

SAXS Study

(ii) sp4+ is a molecular switch triggering the axial curvature of tubulin

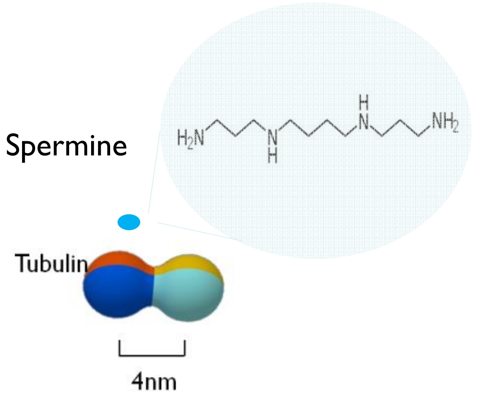

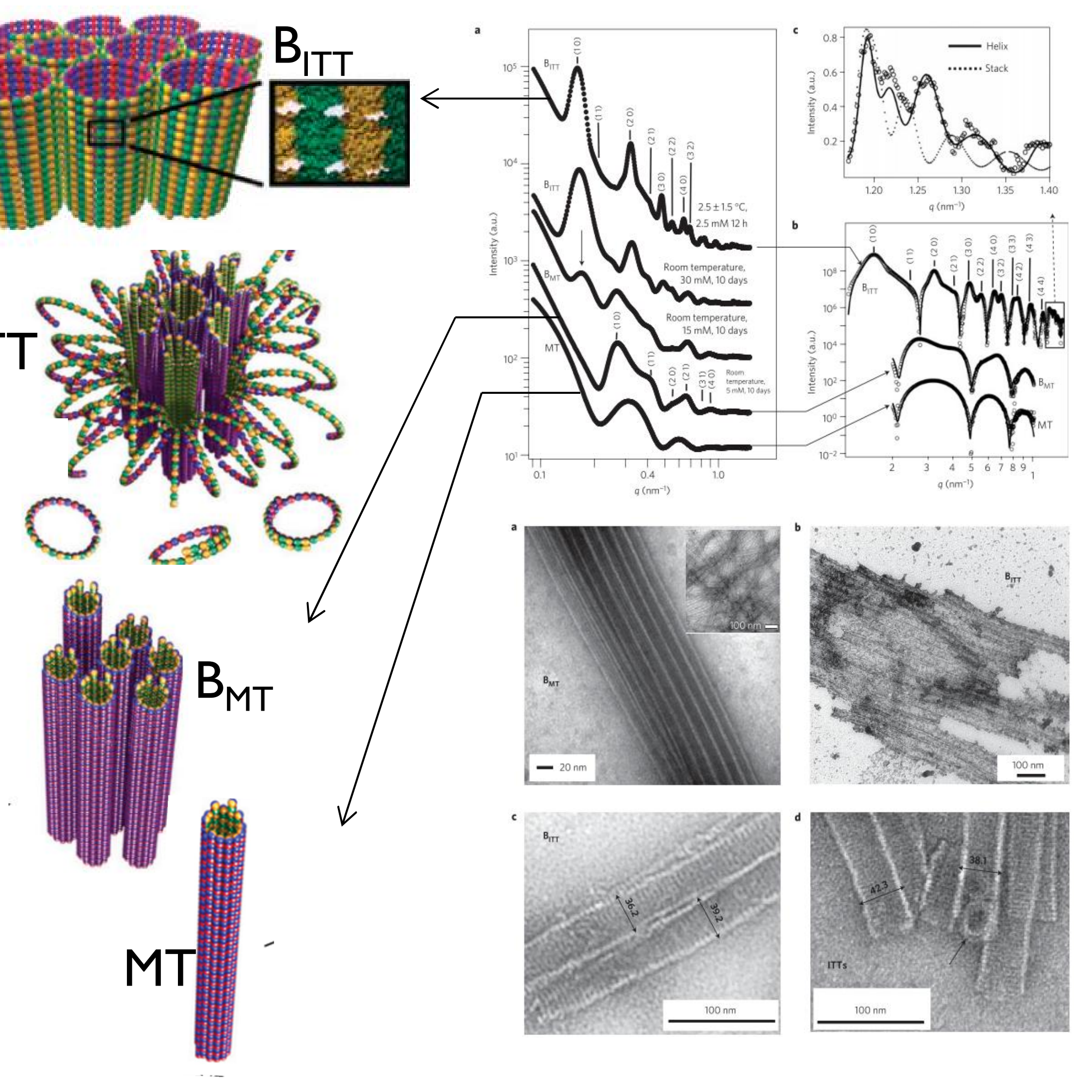

We quantitatively determined the nature of the B_{MT}-to-B_{ITT} transformation pathway, which results from a spermine-triggered conformation switch from straight to curved .

The inverted tubulin columns consist of helical PFs with a tight pitch, not stacks of rings of c-PFs.

M. Ojeda-Lopez, et al., Nature Materials 13 195 (2014)